

See discussions, stats, and author profiles for this publication at: <https://www.researchgate.net/publication/223963776>

# Peptidolipins B–F, Antibacterial Lipopeptides from an Ascidian-Derived *Nocardia* sp.

ARTICLE *in* JOURNAL OF NATURAL PRODUCTS · APRIL 2012

Impact Factor: 3.8 · DOI: 10.1021/np300016r · Source: PubMed

CITATIONS

16

READS

34

5 AUTHORS, INCLUDING:



Tom Wyche

University of Wisconsin–Madison

25 PUBLICATIONS 202 CITATIONS

SEE PROFILE



Yanpeng Hou

PepsiCo Inc.

25 PUBLICATIONS 291 CITATIONS

SEE PROFILE



Emmanuel Vazquez-Rivera

University of Wisconsin–Madison

13 PUBLICATIONS 44 CITATIONS

SEE PROFILE



Tim Bugni

University of Wisconsin–Madison

86 PUBLICATIONS 1,719 CITATIONS

SEE PROFILE

Published in final edited form as:

*J Nat Prod.* 2012 April 27; 75(4): 735–740. doi:10.1021/np300016r.

## Peptidolipins B-F, Antibacterial Lipopeptides from an Ascidian-derived *Nocardia* sp

Thomas P. Wyche, Yanpeng Hou, Emmanuel Vazquez-Rivera, Doug Braun, and Tim S. Bugni\*

Pharmaceutical Sciences Division, University of Wisconsin-Madison, 777 Highland Avenue, Madison, WI, 53705, USA

### Abstract

A marine *Nocardia* sp. isolated from the ascidian *Trididemnum orbiculatum* was found to produce five new lipopeptides, peptidolipins B-F (1–5), which show distinct similarities to the previously reported L-Val(6) analog of peptidolipin NA. Synthetic modification of peptidolipin E (4) was used to determine the location of an olefin within the lipid chain. Advanced Marfey's method was used to determine the absolute configurations of the amino acids. Peptidolipins B (1) and E (4) demonstrated moderate antibacterial activity against methicillin-resistant *Staphylococcus aureus* (MRSA) and methicillin-sensitive *Staphylococcus aureus* (MSSA).

Marine-derived actinomycetes have emerged as a rich source of secondary metabolites with therapeutic relevance.<sup>1</sup> Marine *Nocardia* spp., while not investigated as extensively as other marine actinomycetes, have been a source of antibacterial compounds such as the nocardthiacins,<sup>2</sup> nocardithiocin,<sup>3</sup> and chemomicin A.<sup>4</sup> Among the antibacterial compounds derived from terrestrial isolates of *Nocardia* spp. is the lipopeptide peptidolipin NA.<sup>5</sup> Peptidolipin NA belongs to a rare class of lipopeptides that are characterized by a peptide cyclized via an ester to a lipophilic tail; most lipopeptides, such as daptomycin,<sup>6</sup> do not cyclize through the lipophilic tail. Other members of this class of bacterial-derived compounds have been isolated from *Bacillus subtilis* and include surfactin,<sup>7</sup> iturin A,<sup>8</sup> and bacillomycin D.<sup>9</sup>

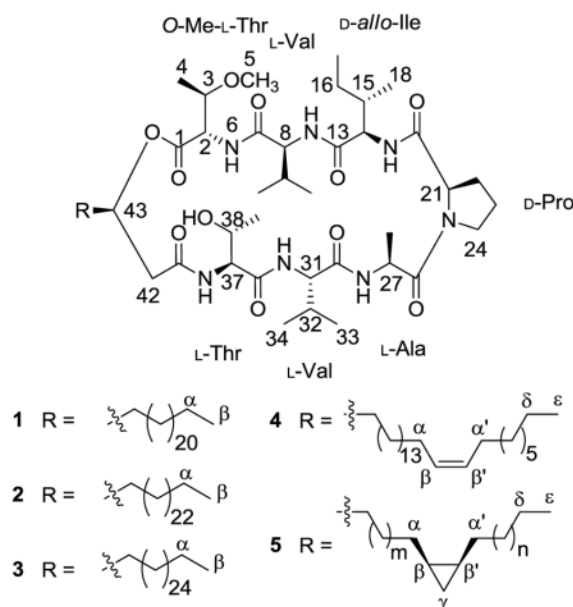
Originally isolated in 1966 from *Nocardia asteroides*,<sup>5</sup> peptidolipin NA and its L-Val(6) analog have demonstrated antibiotic activity and are known to form ion-conducting pores in lipid bilayers.<sup>10</sup> Small molecule interactions with lipid bilayers play an important role in several pharmacologically-relevant processes, such as the detection of specific signaling molecules such as inositol phosphates.<sup>11</sup> Additional studies<sup>12,13</sup> investigating the conformational and self-association properties of peptidolipin NA and its L-Val(6) analog have revealed considerable flexibility within the peptide backbone; the conformation of the peptide backbone depends on the solvent polarity.

Five new lipopeptides, peptidolipins B-F (1–5) were isolated from a marine *Nocardia* sp. (Strain WMMB215), cultivated from the ascidian *Trididemnum orbiculatum* (Van Name, 1902). Peptidolipins B-F (1–5) were deemed similar to the L-Val(6) analog of peptidolipin NA. Each peptide contained a lipid chain; peptidolipin E (4) and F (5) contained an olefin and cyclopropyl group, respectively, within the lipid chain. A combination of NMR, mass

\*To whom correspondence should be addressed: Tel: (608)-263-2519. Fax: (608)-262-5345. tbugni@pharmacy.wisc.edu.

Supporting Information Available. 1D and 2D NMR spectra for compounds 1–5 and molecular modeling data. This material is available free of charge via the Internet at <http://pubs.acs.org>.

spectrometry, synthetic modifications, and molecular modeling led to the elucidation of the structures.



## RESULTS AND DISCUSSION

Strain WMMB215 was selected from 48 marine-derived bacterial extracts, which were analyzed by LCMS, to investigate potentially new chemistry. Strain WMMB215 was found to produce five new lipopeptides, which we named peptidolipins B-F (1–5).

HRMS supported the molecular formula of  $\text{C}_{59}\text{H}_{107}\text{N}_7\text{O}_{11}$  for peptidolipin B (1). Extensive 1D and 2D NMR data (Table 1) were analyzed to establish the peptide backbone and the lactone. In particular, 2D ROESY, COSY, and HMBC NMR data were used to confirm the amino acid sequence (Figure 1). The presence of an *O*-Me threonine at C-5 ( $\delta_{\text{H}}$  3.38) in peptidolipin B (1) was the only difference in the peptide chain when compared to the L-Val(6) analog of peptidolipin NA. The Pro residue was assigned as *trans* based on the  $^{13}\text{C}$  NMR shifts of the  $\beta$ - and  $\gamma$ -carbon atoms ( $\Delta\delta_{\beta\gamma}$ ).  $\Delta\delta_{\beta\gamma}$  for *trans*-Pro is regularly less than 5 ppm while  $\Delta\delta_{\beta\gamma}$  for *cis*-Pro is regularly between 5 and 10 ppm.<sup>14</sup>  $\Delta\delta_{\beta\gamma}$  for the proline residue in 1 was 0.1 ppm, supporting the assignment as *trans*. After determining the peptide portion of peptidolipin B (1), the lipid chain length was confirmed from analysis of the HRMS data.

The advanced Marfey's method<sup>15</sup> was used to determine the absolute configuration of each amino acid. L-FDLA and DL-FDLA were synthesized from 1,5-difluoro-2,4-dinitrobenzene (DFDNB) and L- and DL-leucineamide hydrochloride, respectively.<sup>16</sup> The acid hydrolysate of peptidolipin B (1) was split into two equal portions and derivatized with L-FDLA and DL-FDLA, respectively. LCMS analysis of the L-FDLA and DL-FDLA products supported the assignment of L-Ala, L-Val(2), L-Val(6), and D-Pro. Amino acid standards derivatized with L-FDLA were used for the assignment of L-Thr, *OMe*-L-Thr, and D-*allo*-Ile. The absolute configurations of L-Ala and D-Pro in peptidolipin B (1) differed from the corresponding amino acids in L-Val(6) peptidolipin NA. Minor differences in the  $^1\text{H}$  chemical shifts between L-Val(6) peptidolipin NA and peptidolipin B (1) were observed and prevented us from making any additional conclusions regarding the differences in absolute configuration.

For the known peptidolipins, the absolute configuration at C-43 had not been assigned and prevented any comparisons. Several options were considered for determining the absolute configuration of C-43 in peptidolipin B (**1**). In theory, hydrolysis of the lactone and subsequent esterification using a chiral auxiliary would be sufficient. However, methanolysis of peptidolipin B (**1**) resulted in a complicated  $^1\text{H}$  spectrum with significant peak broadening indicating multiple conformations. The conformational flexibility would preclude the use of a Mosher type method.<sup>17</sup> Complete hydrolysis would provide a secondary alcohol with little distinction among the adjacent methylene proton shifts and would likely not be amenable to a modified Mosher approach. Instead, the chiral BINOL borate method,<sup>18</sup> which compares the chemical shift of the methine hydrogen bonded to the stereogenic carbon, was attempted on the  $\beta$ -hydroxy acid hydrolysate of peptidolipin B (**1**). No change was observed in the  $^1\text{H}$  chemical shifts of H-43 in the *R*- and *S*-BINOL borate derivatives (See Supporting Information), and consequently, another chemical derivatization method was pursued. Lipase B from *Candida antarctica* has been shown to selectively catalyze the hydrolysis of *R*-secondary acetates.<sup>19,20</sup> Methanolysis of peptidolipin B (**1**) followed by acetylation with acetic anhydride in pyridine,<sup>20</sup> resulted in a diacetylated derivative of peptidolipin B (**1**) (See Supporting Information). Addition of lipase B resulted in no reaction of either acetate. The lipophilicity of the diacetate derivative could limit availability of the diacetate derivative to enzymatic hydrolysis. Therefore, several chemical derivatization methods were inconclusive, and a density functional theory (DFT) study was used to assign the absolute configuration of C-43.

Ptak et al. demonstrated that multiple conformations were observed for peptidolipin NA dependent on solvent polarity.<sup>13</sup> The NMR studies on peptidolipin NA demonstrated that peptidolipin NA adopted a stable conformation in pyridine and undergoes self-association in  $\text{CDCl}_3$ . Similarly, different conformations were observed for peptidolipins B-F (**1–5**) in pyridine- $\text{d}_5$  and  $\text{CDCl}_3$ , evidenced by considerable chemical shift differences for amide proton resonances. In pyridine- $\text{d}_5$ , the amide proton resonances showed increased dispersion and were well resolved compared to  $\text{CDCl}_3$  indicating stable hydrogen bonding. These results were in agreement with NMR studies performed on peptidolipin NA and its L-Val(6) analog.<sup>13</sup> Careful analysis of the ROESY spectrum identified key transannular ROEs that would aid with analysis of results from molecular modeling to help confirm that the molecular modeling provided a conformation similar to that observed in pyridine- $\text{d}_5$ .

Models for C-43 *R*- and *S*-peptidolipin B (**1**) were constructed with the lipid chain of peptidolipin B (**1**) truncated to a propyl group to limit conformational flexibility due to the lipid chain. Spartan 10<sup>21</sup> was used to identify the 20 lowest energy conformers for each stereoisomer using a Monte Carlo conformer search with the MMFF force field. For C-43 *R*-peptidolipin B, the three lowest energy conformers accounted for 99.9% of the room temperature populations based on the Boltzmann distribution. The Boltzmann population distribution was 93.9, 3.8, and 2.2%, with energies of 395.4, 403.2, and 404.5 kJ/mol, respectively. Likewise, Boltzmann distribution for the three lowest energy conformers for C-43 *S*-peptidolipin B was 60.2, 22.3, and 8.8%, with energies of 405.0, 407.5, and 409.8 kJ/mol, respectively. The calculated distributions suggested that one major conformer should be observed by  $^1\text{H}$  NMR, paralleled our observation of a stable structure in pyridine, and suggested that a gas phase calculated structure could potentially mimic that observed in pyridine. In parallel with trying to identify the diastereomer that best matched the experimental NMR data, key ROE correlations and coupling constants were used to help confirm that the gas phase model was consistent with the solution structure in pyridine.

The DP4 probability method<sup>22</sup> was used to compare the calculated NMR shifts for the two structures with the observed chemical shifts of peptidolipin B (**1**). For the low energy conformer of each epimer, Gaussian 09<sup>23</sup> was used for geometry optimization and NMR

calculations (B3LYP/6-31G(d,p)).<sup>24</sup> A comparison of the experimental and calculated <sup>13</sup>C NMR shifts with the DP4 probability yielded a 100.0% probability for the *R* configuration compared to the *S* configuration (See Supporting Information). Additionally, key transannular ROE correlations between H-5 and H-40 as well as H-29 and H-19 were examined in each calculated structure. The model of peptidolipin B (**1**) with the *R* configuration at C-43 fit both of these ROE correlations, but the model for the *S*-C-43 did not fit with the correlation between H-5 and H-40. In addition to the ROE correlations, both H-42a and H-42b showed small vicinal <sup>3</sup>J<sub>H</sub> coupling constants of 3.8 Hz to H-43 which is consistent only with the model for C-43 *R*-peptidolipin B (**1**). The model for C-43 *R*-peptidolipin B (**1**) had a dihedral angle of 60.60°, consistent with a small coupling constant, while the model for C-43 *S*-peptidolipin B (**1**) had a dihedral angle of 156.28°, consistent with a large coupling constant.<sup>25</sup> Therefore, the absolute configuration of peptidolipin B (**1**) at C-43 was assigned *R* based on the calculated NMR shifts, ROE correlations, and a vicinal coupling constant.

HRMS supported the molecular formula of C<sub>61</sub>H<sub>111</sub>N<sub>7</sub>O<sub>11</sub> for peptidolipin C (**2**) and C<sub>63</sub>H<sub>115</sub>N<sub>7</sub>O<sub>11</sub> for peptidolipin D (**3**). Extensive analysis of 1D and 2D NMR data (Supporting Information) confirmed that **2** and **3** had the same cyclic peptide structure as peptidolipin B (**1**), and analysis of the HRMS data confirmed that the lipid chain contained two and four additional methylene groups for **2** and **3**, respectively. The absolute configurations in **2** and **3** were assigned the same as **1** due to a shared biogenesis and the identical chemical shifts.

HRMS supported the molecular formula of C<sub>61</sub>H<sub>109</sub>N<sub>7</sub>O<sub>11</sub> for peptidolipin E (**4**) and C<sub>64</sub>H<sub>115</sub>N<sub>7</sub>O<sub>11</sub> for peptidolipin F (**5**). On the basis of 1D and 2D NMR data (Supporting Information) the same cyclic peptide structure as peptidolipins B-D (**1–3**) was confirmed for **4** and **5**. The molecular formula for peptidolipin E (**4**) showed that **4** had an additional degree of unsaturation compared to peptidolipin B (**2**). As supported by chemical shifts of δ<sub>H</sub> 5.52 (H-52, H-53) and δ<sub>C</sub> 130.0 (C-52, C-53), peptidolipin E (**4**) had an olefin within the lipid chain. The olefin was assigned as *Z* based on the <sup>13</sup>C NMR chemical shifts of the allylic carbons.<sup>26</sup> Oxidative cleavage of the double bond in peptidolipin E (**4**) with sodium periodate and osmium tetroxide in aqueous THF formed aldehyde **6**.<sup>27</sup> HRMS supported the molecular formula of C<sub>52</sub>H<sub>91</sub>N<sub>7</sub>O<sub>12</sub> for aldehyde **6** with high mass accuracy (0.1 ppm error), indicating that the double bond was located at C-59 and C-60.

The molecular formula for peptidolipin F (**5**) indicated an additional carbon compared to peptidolipin D (**3**). The 1D NMR spectrum showed a multiplet at –0.19 ppm, characteristic of a diastereotopic hydrogen in a *cis* cyclopropyl group.<sup>28</sup> The geminal diastereotopic hydrogen at 0.68 ppm and adjacent methine protons at 0.75 ppm confirmed the presence of a cyclopropyl group. Previously, the location of cyclopropyl groups in lipid chains was determined by GCMS of picolinyl ester derivatives of cyclopropyl-containing fatty acids.<sup>29,30</sup> Picolinyl esters of cyclopropyl-containing fatty acids showed defined fragmentation patterns when analyzed by GCMS and thus, provided important information for structure determination<sup>29,30</sup> while fragmentation of methyl ester lipids resulted in spectra that were difficult to interpret.<sup>31</sup> An attempt was made to use a similar approach to determine the location of the cyclopropyl group in peptidolipin F (**5**). Hydrolysis of **5** with 6 N HCl at 110 °C for 4 h,<sup>32</sup> and extraction with CHCl<sub>3</sub> provided fatty acid **7**. Esterification of fatty acid **7** with 3-hydroxymethylpyridine under anhydrous conditions formed picolinyl ester **8**. Ester **8** was subjected to GC-MS, but was not detected, potentially due to the large molecular weight of the compound. Ester **8** was observed by MALDI, but MALDI MSMS provided complicated fragmentation that was not useful to identify the location of the cyclopropyl group. In the end, the location of the cyclopropyl group was not determined.

Peptidolipins B-F (1–5) were tested for antibacterial activity against methicillin-sensitive *Staphylococcus aureus* (MSSA) and methicillin-resistant *Staphylococcus aureus* (MRSA), and the minimum inhibitory concentration (MIC) was determined for each compound. Peptidolipins B (1) and E (4) were determined to have an MIC of 64  $\mu\text{g/mL}$  against MSSA and MRSA. Peptidolipins C (2), D (3), and F (5) were determined to have an MIC of greater than 64  $\mu\text{g/mL}$  against MSSA and MRSA. The bioactivity of peptidolipins B (1) and E (4) was similar to the moderate antibacterial activity reported for peptidolipin NA and its L-Val(6) analog.<sup>13</sup> In order to identify if peptidolipins B (1) and E (4) were bactericidal or bacteriostatic, a sterile swab was dipped into each well that showed inhibition of bacterial growth and was inoculated on an LB plate. A bactericidal agent would show no growth on the LB plate while a bacteriostatic agent would show bacterial growth.<sup>33</sup> Therefore, bacterial growth of each sample on the LB plate suggested that peptidolipin B (1) and E (4) are bacteriostatic agents.

Peptidolipins B-F (1–5) were isolated from a marine *Nocardia* sp. and demonstrated conformational flexibility similar to peptidolipin NA and its L-Val(6) analog. Peptidolipins B (1) and E (4) exhibited antibacterial activity against MRSA and MSSA and bacteriostatic action. The long lipophilic tail, containing between 23 and 27 carbons, in peptidolipins B-F (1–5) is unique among lipopeptides. Peptidolipin C (2) was subjected to a SciFinder similarity search to identify known compounds with similar structural features.<sup>34</sup> Of the 8268 compounds identified as having 65–99% similarity to peptidolipin C (2), no compound contained a lipophilic tail with greater than 17 carbons, demonstrating the unique structural features of the isolated compounds.

## EXPERIMENTAL SECTION

### General Experimental Procedures

Optical rotations were measured on a Perkin–Elmer 241 Polarimeter. UV spectra were recorded on an Aminco/OLIS UV-Vis Spectrophotometer. IR spectra were measured with a Bruker Equinox 55/S FT–IR Spectrophotometer. NMR spectra were obtained in pyridine- $d_5$  with a Bruker Avance 600 MHz spectrometer equipped with a 1.7 mm  $^1\text{H}\{^{13}\text{C}/^{15}\text{N}\}$  cryoprobe and a Bruker Avance 500 MHz spectrometer equipped with a  $^{13}\text{C}/^{15}\text{N}\{^1\text{H}\}$  cryoprobe. HRMS data were acquired with a Bruker MaXis 4G QTOF mass spectrometer. RP HPLC was performed using a Shimadzu Prominence HPLC system and a Phenomenex Luna C18 column (250  $\times$  10 mm, 5  $\mu\text{m}$ ). The Advanced Marfey's method utilized a Waters Acquity UPLC coupled with a Bruker MaXis 4G mass spectrometer.

**Biological Material**—Ascidian specimens were collected on October 11, 2010, in the Florida Keys (24° 37.4873, 81° 27.443'). Identification was confirmed by Shirley Parker-Nance. A voucher specimen (FLK10-5-1) for *Trididemnum orbiculatum* (Van Name, 1902) is housed at the University of Wisconsin-Madison. For cultivation, a sample of ascidian (1  $\text{cm}^3$ ) was rinsed with sterile seawater, macerated using a sterile pestle in a micro-centrifuge tube, and dilutions were made in sterile seawater, with vortexing between steps to separate bacteria from heavier tissues. Dilutions were separately plated on three media: ISP2, R2A, and M4. Each medium was supplemented with 50  $\mu\text{g/mL}$  cycloheximide and 25  $\mu\text{g/mL}$  nalidixic acid. Plates were incubated at 28 °C for at least 28 days.

**Sequencing**—16S rDNA sequencing was conducted as previously described.<sup>35</sup> WMMB215 was identified as a *Nocardia* sp. and demonstrated 99% sequence similarity to *Nocardia araeensis* W 9705 (accession number GQ376160.1). The 16S sequence for WMMB215 was deposited in GenBank (accession number JN638997).



**Fermentation, Extraction, and Isolation**—Two 10 mL seed cultures (25 × 150 mm tubes) in medium ASW-A (20 g soluble starch, 10 g glucose, 5 g peptone, 5 g yeast extract, 5 g CaCO<sub>3</sub> per liter of artificial seawater) were inoculated with strain WMMB215 and shaken (200 RPM, 28 °C) for seven days. Two hundred fifty mL baffled flasks (12 × 50 mL) containing ASW-A were inoculated with 1 mL seed culture and were incubated (200 RPM, 28 °C) for seven days. Two-liter flasks (24 × 500 mL) containing medium ASW-A with Diaion HP20 (4% by weight) were inoculated with 25 mL from the 50 mL culture and shaken (200 RPM, 28 °C) for seven days. Filtered HP20 and cells were washed with H<sub>2</sub>O and extracted with acetone. The acetone extract (13.0 g) was subjected to liquid-liquid partitioning using 30% aqueous MeOH and CHCl<sub>3</sub> (1:1). The CHCl<sub>3</sub>-soluble partition (2.2 g) was fractionated by Sephadex LH20 column chromatography (column size CHCl<sub>3</sub>: MeOH, 1:1). Further separation was achieved by silica gel (SiO<sub>2</sub>) column chromatography (10 g, 40–60 μm particle size) with hexanes and isopropanol (0–100%). Fractions containing **1–5**, eluted with 40% isopropanol, were combined and subjected to RP HPLC (2–50% CH<sub>3</sub>CN-CH<sub>2</sub>Cl<sub>2</sub>, 30 min) using a Phenomenex Luna C18 column (250 × 10 mm, 5 μm), yielding **4** (2.0 mg, *t<sub>R</sub>* 25.5 min), **1** (1.8 mg, *t<sub>R</sub>* 26.4 min), **2** (5.5 mg, *t<sub>R</sub>* 28.0 min), **5** (1.1 mg, *t<sub>R</sub>* 28.7 min), and **3** (1.2 mg, *t<sub>R</sub>* 29.3 min).

**Peptidolipin B (1):** white solid; [α]<sub>D</sub><sup>25</sup> +19 (*c* 0.1, CHCl<sub>3</sub>); UV (MeOH) λ<sub>max</sub> (log ε) 213 (4.64) nm; IR (ATR) ν<sub>max</sub> 3279, 2926, 1742, 1641, 1546, 1458 cm<sup>-1</sup>; <sup>1</sup>H and <sup>13</sup>C NMR (See Table 1); HRMS [M+H]<sup>+</sup> *m/z* 1090.8087 (calcd for C<sub>59</sub>H<sub>108</sub> N<sub>7</sub>O<sub>11</sub>, 1090.8101).

**Peptidolipin C (2):** white solid; [α]<sub>D</sub><sup>25</sup> +21 (*c* 0.5, CHCl<sub>3</sub>); UV (MeOH) λ<sub>max</sub> (log ε) 210 (4.43) nm; IR (ATR) ν<sub>max</sub> 3284, 2926, 1738, 1646, 1544, 1462 cm<sup>-1</sup>; <sup>1</sup>H and <sup>13</sup>C NMR (See Table S3); HRMS [M+H]<sup>+</sup> *m/z* 1118.8407 (calcd for C<sub>61</sub>H<sub>112</sub> N<sub>7</sub>O<sub>11</sub>, 1118.8414).

**Peptidolipin D (3):** white solid; [α]<sub>D</sub><sup>25</sup> +4.4 (*c* 0.1, CHCl<sub>3</sub>); UV (MeOH) λ<sub>max</sub> (log ε) 212 (4.83) nm; IR (ATR) ν<sub>max</sub> 3278, 2928, 1743, 1643, 1543, 1464 cm<sup>-1</sup>; <sup>1</sup>H and <sup>13</sup>C NMR (See Table S3); HRMS [M+H]<sup>+</sup> *m/z* 1146.8702 (calcd for C<sub>63</sub>H<sub>116</sub> N<sub>7</sub>O<sub>11</sub>, 1146.8727).

**Peptidolipin E (4):** white solid; [α]<sub>D</sub><sup>25</sup> +20 (*c* 0.2, CHCl<sub>3</sub>); UV (MeOH) λ<sub>max</sub> (log ε) 213 (4.60) nm; IR (ATR) ν<sub>max</sub> 3283, 2928, 1742, 1639, 1541, 1460 cm<sup>-1</sup>; <sup>1</sup>H and <sup>13</sup>C NMR (See Table S4); HRMS [M+H]<sup>+</sup> *m/z* 1116.8233 (calcd for C<sub>61</sub>H<sub>110</sub> N<sub>7</sub>O<sub>11</sub>, 1116.8258).

**Peptidolipin F (5):** white solid; [α]<sub>D</sub><sup>25</sup> +6.4 (*c* 0.09, CHCl<sub>3</sub>); UV (MeOH) λ<sub>max</sub> (log ε) 211 (4.51) nm; IR (ATR) ν<sub>max</sub> 3287, 2926, 1735, 1648, 1542, 1460 cm<sup>-1</sup>; <sup>1</sup>H and <sup>13</sup>C NMR (See Table S4); HRMS [M+H]<sup>+</sup> *m/z* 1158.8707 (calcd for C<sub>64</sub>H<sub>116</sub> N<sub>7</sub>O<sub>11</sub>, 1158.8727).

**Molecular Modeling Calculations**—Molecular modeling calculations were performed on a Dell Precision T5500 Linux workstation with a Xeon processor (3.3 GHz, 6-core). Low energy conformers were obtained using Spartan 10 software (MMFF, 10000 conformers examined). The low energy conformer for each compound was analyzed using Gaussian 09 for geometry optimization and NMR calculations (B3LYP/6-31G(d,p)). NMR shifts were referenced to TMS and benzene using the multi-standard (MSTD) approach.<sup>36</sup> Molecules were modeled in the gas phase.

**Determination of Amino Acid Configurations**—L- and DL-FDLA were synthesized as previously reported.<sup>16</sup> Peptidolipin B (**1**) (0.3 mg) was hydrolyzed with 6 N HCl (1 mL) for 4 h at 110 °C and dried under vacuum. The acid hydrolysate was dissolved in 100 μL H<sub>2</sub>O and split into two equal portions. Each portion was mixed with 1 N NaHCO<sub>3</sub> (20 μL), acetone (110 μL), and 20 μL of L- or DL-FDLA (10 mg/mL in acetone). Each solution was stirred for 1 h at 40 °C. The reaction was quenched with 1 N HCl (20 μL) and dried under

vacuum. A portion of each product was dissolved in MeOH:H<sub>2</sub>O (1:1) for LCMS analysis. Separation of the derivatives was achieved with a Phenomenex Kinetex C18 reversed-phase column (2.6  $\mu$ m, 150  $\times$  2.0 mm) at a flow rate of 0.2 mL/min and with a linear gradient of H<sub>2</sub>O (containing 0.1% formic acid) and MeOH (90:10 to 3:97 over 29 min). The absolute configurations of the amino acids were determined by comparing the retention times of the L- and DL-FDLA derivatives, which were identified by MS. Retention times of the DL-FDLA amino acid derivatives were 13.7 and 19.0 min (Ala), 13.2 and 15.7 min (Val), and 9.6 and 12.7 min (Pro). The retention times of the L-FDLA amino acid derivatives were 13.8 (L-Ala), 13.2 (L-Val(2) and L-Val (6)), and 12.3 min (D-Pro). The absolute configurations of the remaining amino acids were assigned based on a comparison of retention time of amino acid standards (L-Thr, D-*allo*-Ile, and OMe-L-Thr) derivatized with L-FDLA. The retention times of L-FDLA derivatives of the acid hydrolysate and the amino acid standards were identified at 11.2 (L-Thr), 11.9 (OMe-L-Thr), and 16.5 min (D-*allo*-Ile). The amino acids were assigned as L-Thr, L-Val(2), L-Ala, D-Pro, D-*allo*-Ile, L-Val(6), and OMe-L-Thr.

**Aldehyde 6**—Compound **4** (500  $\mu$ g) was dissolved in THF and H<sub>2</sub>O (1:1 v/v, 2 mL). While stirring, 60 mg NaIO<sub>4</sub> was added to the solution. OsO<sub>4</sub> (0.84 mg in H<sub>2</sub>O) was slowly added to the solution. The solution was stirred at room temperature (rt) for 1 h. THF was removed using rotary evaporation, and the remaining aqueous phase was extracted twice with CH<sub>2</sub>Cl<sub>2</sub>. The CH<sub>2</sub>Cl<sub>2</sub> portions were dried using rotary evaporation to yield about 300  $\mu$ g of crude product, containing aldehyde **6**. The crude product was analyzed by <sup>1</sup>H NMR and HRESIMS to determine the structure of **6**. **6**: HRMS *m/z* 1006.6797 [M+H]<sup>+</sup> (calcd for C<sub>52</sub>H<sub>92</sub>N<sub>7</sub>O<sub>12</sub>, 1006.6798).

**Ester 8**—Compound **5** (500  $\mu$ g) was dissolved in 6 N HCl (2 mL) and stirred at 120 °C for 4 h. After 4 h, the solution was cooled to rt and extracted with CHCl<sub>3</sub>. The CHCl<sub>3</sub> layer was dried in vacuo to yield acid **7**. Acid **7** was dissolved in dry CH<sub>2</sub>Cl<sub>2</sub> (500  $\mu$ L) and added to a solution containing potassium *t*-butoxide (1.0 M) in THF (50  $\mu$ L) and 3-hydroxymethylpyridine (100  $\mu$ L). The mixture was held at 45 °C for 45 min. After 45 min, the reaction mixture was cooled to rt. H<sub>2</sub>O (0.5 mL) and hexanes (1 mL) were added and vortexed. The organic phase was collected and dried under argon to yield ester **8**.

**Antibacterial Assay**—Peptidolipins B-F (**1–5**) were tested for antibacterial activity against MSSA (ATCC #29213) and MRSA (ATCC #33591), and MICs were determined using a dilution antimicrobial susceptibility test for aerobic bacteria.<sup>37</sup> Peptidolipins B-F (**1–5**) were dissolved in DMSO, serially diluted to 10 concentrations (0.125 – 64  $\mu$ g/mL), and tested in a 96-well plate. Vancomycin was used as a control and exhibited an MIC of 1  $\mu$ g/mL against MSSA and 1  $\mu$ g/mL against MRSA. Peptidolipins B-F (**1–5**) were tested in triplicate, and vancomycin was tested in triplicate. Six untreated media controls were included on each plate. The plates were incubated at 33 °C for 18 h. The MIC was determined as the lowest concentration that inhibited visible growth of bacteria.

## Supplementary Material

Refer to Web version on PubMed Central for supplementary material.

## Acknowledgments

This work was supported by funding from the University of Wisconsin-Madison School of Pharmacy, the Graduate School at the University of Wisconsin, and the UW College of Agriculture and Life Sciences. This work was also funded by the NIH, NIGMS Grant R01 GM092009. We would like to thank the Analytical Instrumentation Center at the University of Wisconsin-Madison for the facilities to acquire spectroscopic data, as well as Dr. M. Vestling



and Dr. R. McClain for instrumentation in the Department of Chemistry. This study made use of the National Magnetic Resonance Facility at Madison, which is supported by NIH grants P41RR02301 (BRTP/NCRR) and P41GM66326 (NIGMS). Additional equipment was purchased with funds from the University of Wisconsin, the NIH (RR02781, RR08438), the NSF (DMB-8415048, OIA-9977486, BIR-9214394), and the USDA. We would like to thank D. Demaria for assistance with collection, S. Parker-Nance for taxonomy, and Dr. W. Rose for assistance with the antibacterial assays.

## References

1. Fenical W, Jensen PR. *Nat Chem Biol.* 2006; 2:666–673. [PubMed: 17108984]
2. Li W, Leet JE, Ax HA, Gustavson DR, Brown DM, Turner L, Brown K, Clark J, Yang H, Fung-Tomc J, Lam KS. *J Antibiot.* 2003; 56:226–231. [PubMed: 12760678]
3. Mukai A, Fukai T, Hoshino Y, Yazawa K, Harada K, Mikami Y. *J Antibiot.* 2009; 62:613–619. [PubMed: 19745839]
4. Sun C, Wang Y, Wang Z, Zhou J, Jin W, You X, Gao H, Zhao L, Si S, Li X. *J Antibiot.* 2007; 60:211–215. [PubMed: 17446695]
5. Guinand M, Michel G. *Biochim Biophys Acta.* 1966; 125:75–91. [PubMed: 5968596]
6. Eliopoulos GM, Willey S, Reiszner E, Spitzer PG, Caputo G, Moellering RC. *Antimicrob Agents Chemother.* 1986; 30:532–535. [PubMed: 3024560]
7. Arima K, Kakinuma A, Tamura G. *Biochem Biophys Res Commun.* 1968; 31:488–94. [PubMed: 4968234]
8. Delcambe L, Peypoux F, Besson F, Guinand M, Michel G. *Biochem Soc Trans.* 1977; 5:1122–1124. [PubMed: 913800]
9. Peypoux F, Besson F, Michel G, Delcambe L. *Eur J Biochem.* 1981; 118:323–327. [PubMed: 7285926]
10. Maget-Dana R, Heitz F, Ptak M, Peypoux F, Guinand M. *Biochem Biophys Res Commun.* 1985; 129:965–971. [PubMed: 2409974]
11. Scheidt HA, Huster D. *Acta Pharmacol Sin.* 2008; 29:35–49. [PubMed: 18158864]
12. Ptak M, Heitz A, Guinand M, Michel G. *Biochem Biophys Res Commun.* 1980; 94:1311–1318. [PubMed: 7396964]
13. Ptak M, Heitz A, Guinand M, Michel G. *Int J Biol Macromol.* 1982; 4:79–90.
14. Siemion IZ, Wieland T, Pook KH. *Angew Chem Int Ed.* 1975; 14:702–703.
15. Fujii K, Ikai Y, Oka H, Suzuki M, Harada K. *Anal Chem.* 1997; 69:5146–5151.
16. Marfey P. *Carlsberg Res Commun.* 1984; 49:591–596.
17. Dale JA, Mosher HS. *J Am Chem Soc.* 1973; 95:512–519.
18. Freire F, Quiñoá E, Riguera R. *Chem Commun.* 2008; 4147–4149.
19. Ohtanib T, Nakatsukasaa H, Kamezawab M, Tachibanab H, Naoshimaa Y. *J Mol Catal B: Enzym.* 1998; 4:53–60.
20. Whitson EL, Ratnayake AS, Bugni TS, Harper MK, Ireland CM. *J Org Chem.* 2009; 74:1156–1162. [PubMed: 19053188]
21. Deppmeier, BJ.; Driessen, AJ.; Hehre, TS.; Hehre, WJ.; Johnson, JA.; Klunzinger, PE.; Leonard, JM.; Ohlinger, WS.; Pham, IN.; Pietro, WJ.; Yu, J. *Spartan 10. Vol. 1.0.2. Wavefunction Inc;* Irvine, CA: 2011.
22. Smith SG, Goodman JM. *J Am Chem Soc.* 2010; 132:12946–12959. [PubMed: 20795713]
23. Frisch, MJ.; Trucks, GW.; Schlegel, HB.; Scuseria, GE.; Robb, MA.; Cheeseman, JR.; Scalmani, G.; Barone, V.; Mennucci, B.; Petersson, GA.; Nakatsuji, H.; Caricato, M.; Li, X.; Hratchian, HP.; Izmaylov, AF.; Bloino, J.; Zheng, G.; Sonnenberg, JL.; Hada, M.; Ehara, M.; Toyota, K.; Fukuda, R.; Hasegawa, J.; Ishida, M.; Nakajima, T.; Honda, Y.; Kitao, O.; Nakai, H.; Vreven, T.; Montgomery, JA., Jr; Peralta, JE.; Ogliaro, F.; Bearpark, M.; Heyd, JJ.; Brothers, E.; Kudin, KN.; Staroverov, VN.; Kobayashi, R.; Normand, J.; Raghavachari, K.; Rendell, A.; Burant, JC.; Iyengar, SS.; Tomasi, J.; Cossi, M.; Rega, N.; Millam, NJ.; Klene, M.; Knox, JE.; Cross, JB.; Bakken, V.; Adamo, C.; Jaramillo, J.; Gomperts, R.; Stratmann, RE.; Yazyev, O.; Austin, AJ.; Cammi, R.; Pomelli, C.; Ochterski, JW.; Martin, RL.; Morokuma, K.; Zakrzewski, VG.; Voth,

- GA.; Salvador, P.; Dannenberg, JJ.; Dapprich, S.; Daniels, AD.; Farkas, Ö.; Foresman, JB.; Ortiz, JV.; Cioslowski, J.; Fox, DJ. Gaussian 09, Revision A.1. Gaussian, Inc; Wallingford CT: 2009.
24. Stappen I, Buchbauer G, Robien W, Wolschann P. Magn Reson Chem. 2009; 47:720–726. [PubMed: 19475540]
25. Karplus M. J Am Chem Soc. 1963; 85:2870–2871.
26. Carpita A, Quirici MG, Veracini CA. Tetrahedron. 1982; 38:639–644.
27. Rappo R, Allen DS Jr, Lemieux U, Johnson WS. J Org Chem. 1956; 21:478–479.
28. Knothe G. Lipids. 2006; 41:393–396. [PubMed: 16808153]
29. Destailats F, Angers P. J Am Oil Chem Soc. 2002; 79:253–256.
30. Harvey DJ. Biomed Mass Spectrom. 1984; 11:187–192.
31. Hanus LO, Goldshlag P, Dembitsky VM. Biomed Pap Med Fac Univ Palacky Olomouc Czech Repub. 2008; 152:41–45. [PubMed: 18795073]
32. Laird DW, LaBarbera DV, Feng X, Bugni TS, Harper MK, Ireland CM. J Nat Prod. 2007; 70:743–746.
33. Pankey GA, Sabath LD. Clin Infect Dis. 2004; 38:864–870. [PubMed: 14999632]
34. *SciFinder*, version 2011.1. Chemical Abstracts Service; Columbus, OH: 2011.
35. Wyche TP, Hou Y, Braun D, Cohen HC, Xiong MP, Bugni TS. J Org Chem. 2011; 76:6542–6547. [PubMed: 21736356]
36. Sarow AM, Pellegrinet SC. J Org Chem. 2009; 74:7254–7260. [PubMed: 19725561]
37. National Committee for Clinical Laboratory Standards. Methods for Dilution Antimicrobial Susceptibility Tests for Bacteria that Grow Aerobically. 7. NCCLS; Villanova, PA: 2006. Approved standard M7-A7

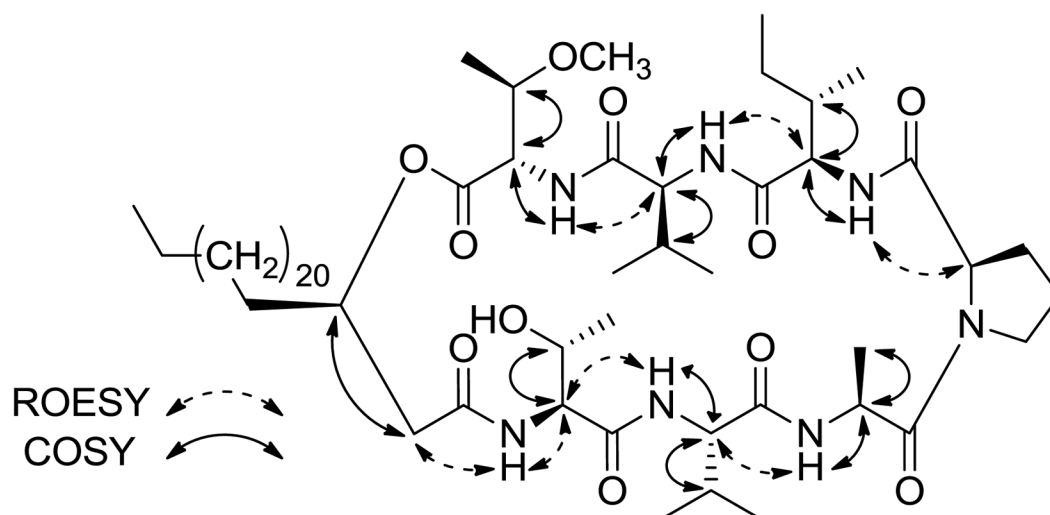
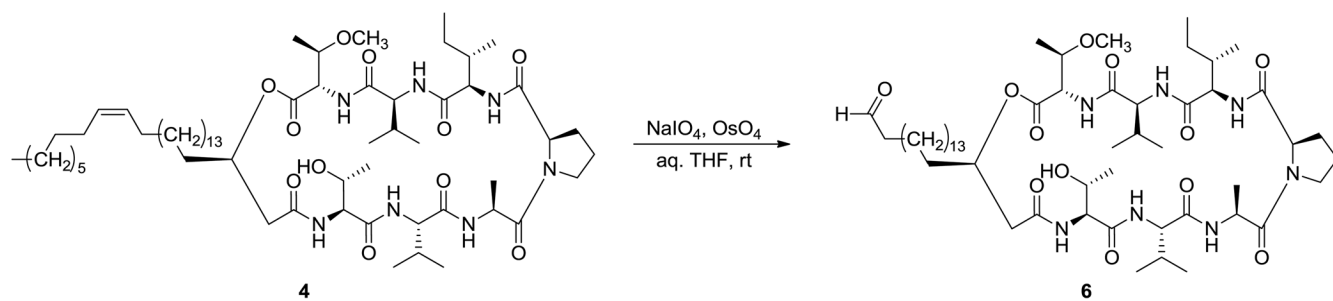
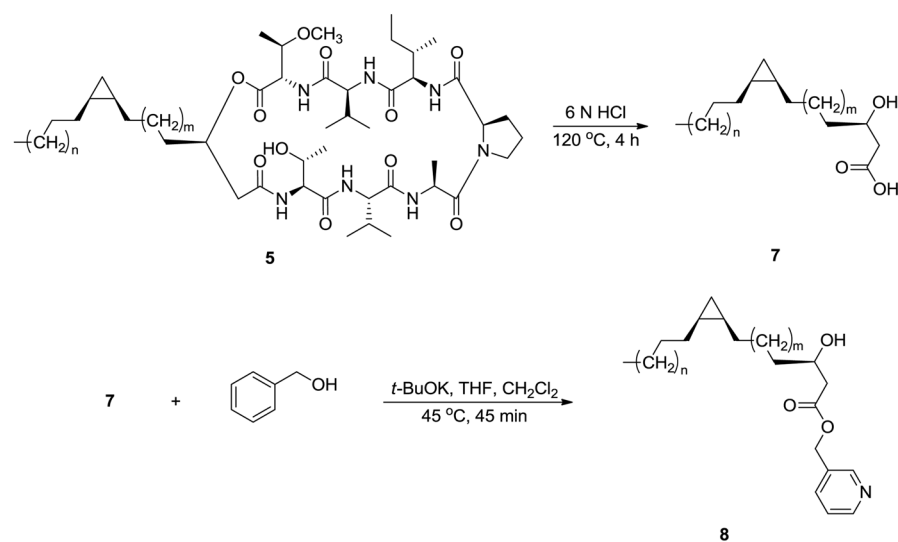


**Figure 1.**  
Key ROESY and COSY correlations for **1**



**Scheme 1.**  
Oxidation of **4**



**Scheme 2.**  
Hydrolysis and Esterification of 5

TABLE 1

<sup>1</sup>H and <sup>13</sup>C NMR Data for 1 (600 MHz for <sup>1</sup>H, 150 MHz for <sup>13</sup>C, pyridine-d<sub>5</sub>)

Position	$\delta_C$ , mult.	$\delta_H$ (J in Hz)	COSY	HMBC
1	170.9, C			
2	57.2, CH	5.35, m	3, 6	1
3	79.7, CH	4.16, m	2, 4	
4	14.3, CH <sub>3</sub>	1.09, d (6.0)	3	
5	56.7, CH <sub>3</sub>	3.38, s		
6-NH		9.46, d (10.2)	2	7
7	172.1, C			
8	59.0, CH	5.55, t (8.7)	12, 9	7, 9, 10, 11
9	32.8, CH	2.48, m	8, 10, 11	
10	19.83, CH <sub>3</sub>	1.31, m	9	8
11	19.80, CH <sub>3</sub>	1.28, m	9	8
12-NH		9.31, d (8.7)	8	13
13	173.4, C			
14	57.3, CH	5.07, m	15, 19	18
15	37.6, CH	2.13, m	14, 18	
16	27.5, CH <sub>2</sub>	1.54, m	17	14, 15
		1.31, m		
17	11.8, CH <sub>3</sub>	0.80, t (7.5)	16	15, 16
18	14.5, CH <sub>3</sub>	1.15, d (6.8)	15	14, 15, 16
19-NH		8.31, d (9.0)	18	
20	172.4, C			
21	58.9, CH	5.05, m		20, 22, 24
22	24.7, CH <sub>2</sub>	2.52, m	23	24
		1.54, m		
23	24.8, CH <sub>2</sub>	2.01, m	22, 24	
		1.70, m		
24	46.2, CH <sub>2</sub>	3.45, m	23	23
		3.40, m		
26	172.17, C			
27	48.3, CH	5.04, m	28, 29	26, 28
28	17.0, CH <sub>3</sub>	1.68, d (6.4)	27	26, 27
29-NH		8.85, d (6.4)	27	27, 30
30	172.19, C			
31	59.2, CH	5.25, t (9.0)	32, 35	30, 32, 33
32	32.2, CH	2.31, m	31, 33, 34	31, 33
33	19.6, CH <sub>3</sub>	1.19, d (6.8)	32	31, 32, 34
34	20.1, CH <sub>3</sub>	1.24, m	32	31, 32, 33
35-NH		10.15, d (9.4)	31	36



Position	$\delta_C$ , mult.	$\delta_H$ (J in Hz)	COSY	HMBC
36	171.9, C			
37	59.5, CH	5.38, m	38, 40	36, 38, 39
38	68.2, CH	4.45, m	37, 39	
38-OH		6.79, d (5.3)	38	
39	20.4, CH <sub>3</sub>	1.46, d (6.0)	38	37, 38
40-NH		7.72, d (8.7)	37	41
41	169.6, C			
42	41.4, CH <sub>2</sub>	2.89, dd (13.6, 3.8) 2.59, dd (13.6, 3.8)	43	41, 43, 44
43	72.6, CH	5.40, m	42, 44	
44	32.5, CH <sub>2</sub>	1.87, m 1.82, m	43, 45	43
45	32.1, CH <sub>2</sub>	1.23, m	44	
46–64	30.0–30.4, CH <sub>2</sub>	1.2–1.4, m		
$\alpha$	23.1, CH <sub>2</sub>	1.25, m		$\beta$
$\beta$	14.4, CH <sub>3</sub>	0.88, t (6.4)		$\alpha$